Published in final edited form as:
Anal Chem. 2013 July 16; 85(14): 6732–6739. doi:10.1021/ac4012232.

A Quantitative Mass Spectrometry-Based Approach for Assessing the Repair of 8-Methoxypsoralen-Induced DNA Interstrand Crosslink and Monoadducts in Mammalian Cells

Shuo Liu[1] and **Yinsheng Wang**[1,2,*]

[1]Environmental Toxicology Graduate Program, University of California, Riverside, California 92521

[2]Department of Chemistry, University of California, Riverside, California 92521

Abstract

Interstrand crosslinks (ICLs) are highly toxic DNA lesions that block transcription and replication by preventing strand separation. ICL-inducing agents were among the earliest, and are still the most widely used, forms of chemotherapeutic drugs. Owing to the repair of DNA ICLs, the therapeutic efficacy of the DNA crosslinking agents is often set back by the development of chemoresistance in patients. Thus, it is very important to understand how various DNA ICLs are repaired. Such studies are currently hampered by the lack of an analytical method for monitoring directly the repair of DNA ICLs in cells. Here we report an HPLC coupled with tandem mass spectrometry (LC-MS/MS) method, together with the isotope dilution technique, for assessing the repair of 8-methoxypsoralen (8-MOP)-induced DNA ICL, as well as monoadducts (MAs), in cultured mammalian cells. We found that, while there were substantial decreases in the levels of ICL and MAs in repair-competent cells at 24 hr after 8-MOP/UVA treatment, there were little repair of 8-MOP-ICL and MAs in XPA-deficient human skin fibroblasts and ERCC1-deficient Chinese hamster ovary (CHO) cells over a 24-hr period. This result provided unequivocal evidence to support that the 8-MOP photoadducts are substrates for nucleotide excision repair (NER) in mammalian cells. This is one of the first few reports about the application of LC-MS/MS for assessing the repair of DNA ICLs. The analytical method developed here, when combined with genetic manipulation, will also facilitate the assessment about the roles of other DNA repair pathways in removing these DNA lesions, and the method can also be generally applicable for investigating the repair of other types of DNA ICLs in mammalian cells.

Introduction

DNA in eukaryotic cells is constantly damaged through exposure to a variety of reactive chemicals derived from external and internal sources.[1, 2] It was estimated that tens of thousands of DNA lesions can be induced in each of the ~10^{13} cells in the human body per day.[1, 3] Because damage to DNA may be incompatible with its essential roles in preservation and transmission of genetic information, multiple DNA repair pathways have evolved in organisms to maintain genomic stability and cell viability. These include, but are not limited to, nucleotide excision repair (NER), mismatch repair (MMR), base excision repair (BER) and recombinational repair.[2] If left unrepaired, DNA damage may perturb the

*To whom correspondence should be addressed: Department of Chemistry-027, University of California, Riverside, CA 92521-0403. Telephone: (951) 827-2700. Fax: (951) 827-4713. yinsheng.wang@ucr.edu.

Supporting Information

HPLC trace for the separation of ICL- and MA-containing ODNs, calibration curves for quantification, and levels of 8-MOP-ICL and -MAs in HEK293T cells. This material is available free of charge via the Internet at http://pubs.acs.org.

flow of genetic information by inhibiting DNA replication and transcription and by inducing mutations during these processes, which may ultimately lead to the development of cancer, neurodegeneration, or other human diseases.[2]

DNA interstrand crosslink (ICL) is among the most toxic type of DNA lesions.[4] It has been estimated that a single ICL can kill a repair-deficient bacterial or yeast cell, and as few as 20–40 ICLs can be lethal to a mammalian cell lacking the ability to remove the crosslink.[5, 6] Because of the presence of covalent linkages between the opposing strands of DNA, ICLs may completely block replication and transcription, and consequently pose a formidable challenge to cell survival and to the maintenance of genetic information.[7, 8] On the other hand, it is also this cytotoxic effect that constitutes the mechanistic basis of action for many currently used cancer chemotherapeutic agents.[9]

Psoralen and its derivatives, a group of furocoumarins naturally found in leafy vegetables and other plants, are well-known bifunctional photoreactive DNA crosslinking agents. Upon long-wavelength UV irradiation, psoralen reacts preferentially with thymine residue at 5′-TpA site to form monoadducts (MAs) or interstrand crosslink via [2+2] cycloaddition.[10] Psoralen plus UVA (PUVA) is a widely used and effective therapy for several hyper-proliferative skin disorders such as psoriasis and vitiligo[11] and has been used for the treatment of cutaneous T-cell lymphoma.[12] The effectiveness of PUVA treatment is largely attributed to the formation of DNA ICLs. However, the benefit of PUVA treatment is accompanied with the risk of developing non-melanoma skin cancer.[13] Thus, a better understanding of the repair of psoralen-photoactivated ICL will provide important knowledge for developing improved PUVA therapies for the treatment of cancer and other human diseases.

Owing to the different properties of ICLs and depending on the cell cycle phase, ICLs are most likely processed through multiple repair mechanisms *in vivo*.[9] A conceptual model consisting of a two-cycle scheme has been proposed for ICL repair. The first cycle is thought to begin with the cleavage of one strand on both the 5′ and 3′ sides of the damaged base by NER enzymes, resulting in the generation of a gapped intermediate.[14] Gap filling is executed by translesion synthesis in non-dividing cells or by recombination repair in actively dividing cells using the undamaged homologous chromosome as the template.[15] The gap-filling process converts an ICL into an MA, after which the second cycle of excision repair removes the MA presumably through the conventional NER pathway.[5] The above scheme has delineated a general mechanism for ICL repair in *E. coli* and yeast. However, our understanding about the repair of ICLs in mammalian cells is far from complete.

Assessing the repair of DNA ICLs often necessitates the measurement of the levels of these lesions in cells and tissues. Several biophysical and biochemical techniques have been used for measuring ICLs, which include agarose gel-based method,[16] alkaline filter elution,[17] alkaline comet assay,[18] and chromatographic techniques.[19] A drawback of these methods is their relatively low sensitivity or a requirement for a high level of ICL, which is lethal to almost all cells and may saturate cellular DNA repair capacity. Additionally, these methods do not provide structural information about the ICLs. With the development and application of mass spectrometry techniques, the detection sensitivity of DNA damage analysis has been greatly improved. By using HPLC coupled with tandem mass spectrometry (LC-MS/MS), Courdavault et al.[20] studied the repair of three types of bipyrimidine photoproducts in keratinocytes, where they observed a rapid elimination of TT-(6–4) photoproduct from cellular DNA 72 hr post-irradiation. With the use of inductively coupled plasma mass spectrometry (ICP-MS), Harrington et al.[21] discovered a faster removal of cisplatin 1,2-intrastrand guanine-guanine adducts (1,2-GG) in cisplatin-resistant human lung tumor cells

relative to drug-sensitive cells. LC-MS/MS/MS with the isotope-dilution technique has also been employed to examine the role of NER in repairing endogenously induced intrastrand crosslink d(G[8–5m]T), 8,5′-cyclo-2′-deoxyadenosine, and 8,5′-cyclo-2′-deoxyguanosine in mammalian tissues.[22, 23]

We recently reported the application of LC-MS/MS in assessing the levels of ICLs and MAs formed in human cells upon exposure to different psoralen derivatives.[24, 25] LC-MS/MS, however, has been rarely employed for examining the repair of DNA ICLs. In this vein, considering the high cytotoxicity of DNA ICLs, it is potentially challenging to identify an experimental condition that can allow for the generation of adequate level of DNA ICLs for LC-MS/MS detection without compromising the repair capacity or survival of the host cells. Malayappan et al.[26] used LC-MS/MS to follow the formation and repair of cyclophosphamide-induced *N,N*-bis[2-(*N*7-guanyl)ethyl]amine crosslink in human blood, but intrastrand and interstrand crosslinks were not distinguished in that study because both types of lesions were released as free base adducts after neutral thermal hydrolysis. It was also reported that ICLs introduced by mitomycin C could be partially removed in mouse mammary tumor cells.[27] However, a crosslinked dinucleoside standard was used for the quantitative measurement. Given that the release of mitomycin C interstrand crosslink from genomic DNA may not be complete, the accuracy for the quantification remains uncertain.

Herein, we demonstrated the capability of LC-MS/MS in assessing directly the repair of 8-MOP-induced DNA ICL, as well as MAs, in mammalian cells. Moreover, our results provided unequivocal evidence to support that NER functions in repairing the 8-MOP-induced ICL and MAs in mammalian cells.

Experimental Section

Materials and Cell Lines

All chemicals and enzymes, unless otherwise specified, were from Sigma-Aldrich (St. Louis, MO) and New England Biolabs (Ipswich, WA). All oligodeoxyribonucleotides (ODNs) used in this study were purchased from Integrated DNA Technologies (Coralville, IA). [8-D_3]-8-methoxypsoralen (D_3-8-MOP) was synthesized previously.[24]

Human embryonic kidney 293T cells (HEK293T) were obtained from the American Type Culture Collection (Manassas, VA). Human skin fibroblasts (HFs) that are repair-competent (GM00637) or deficient in xeroderma pigmentosum complementation group A (XPA, GM04429) were provided by Prof. Gerd P. Pfeifer (City of Hope). Repair-proficient AA8 Chinese hamster ovary (CHO) cells and the isogenic CHO cells that are deficient in excision repair cross-complementing rodent repair deficiency, complementation group 1 (ERCC1, CHO-7–27)[28] were provided by Prof. Michael M. Seidman (National Institute of Aging).

Preparation of Standard ICL- and MA-Containing ODNs

ODNs containing an ICL or MA introduced by 8-methoxypsoralen (8-MOP) or D_3-8-MOP were prepared following the previously reported procedures with modifications.[24] Structures of unlabeled and labeled 8-MOP are depicted in Scheme 1A. A 10-nmol self-complementary ODN d(CGCGCTAGCGCG) was annealed in a 40-μL reaction buffer that contained 5 mM Tris (pH 7.6), 50 mM NaCl and 0.2 mM EDTA. The ODN solution was diluted to 1 mL with the reaction buffer, and a solution of 8-MOP or D_3-8-MOP in ethanol was added until its final concentration reached 1 mM. The reaction mixture was subsequently dispersed in a 3.5-cm-i.d. Petri dish and incubated in the dark for 1 hr. The resulting solution was irradiated on ice for 45 min with UVA light, which was delivered by two 15-W Spectroline light tubes with emitting wavelength centered at 365 nm (Spectronics Corp., Westbury, NY). The irradiation mixture, which contained both ICLs and unreacted starting material,

was immediately irradiated on ice with short-wavelength UV light centered at 254 nm (Spectronics Corp.) for 15 sec to facilitate the photo-reversal of ICL-containing ODNs.[25] After irradiation, the solution was extracted with chloroform, and the ODNs were recovered by ethanol precipitation, separated by HPLC, and used as standards for LC-MS/MS analysis.

HPLC Conditions

The purification of ICL- and MA-containing ODNs was performed on an Agilent 1100 HPLC system with a UV detector monitoring at 260 nm. A 4.6×150 mm Aeris WIDEPORE column (3.6 μm in particle size and 200 Å in pore size, Torrance, CA) was used, and the column was heated to 50°C by using an SP8790 column heater (Spectra Physics, San Jose, CA). A solution of 50 mM triethylammonium acetate (TEAA, pH 6.8) and a solution of 30% (v/v) acetonitrile in 50 mM TEAA were used as mobile phases A and B, respectively. A gradient of 5 min 0–25% B and 40 min 25–50% B was employed, and the flow rate was 0.8 mL/min. The purities of the ICL- and MA-containing ODNs were verified by LC-MS/MS analysis.

Cell Culture and Drug Treatment

Cells were routinely cultured at 37°C in 5% CO_2 atmosphere. Human skin fibroblasts and HEK293T cells were grown in Dulbecco's Modified Eagle Medium, and CHO cells were grown in Alpha Minimum Essential Medium without ribonucleosides or deoxyribonucleosides. All culture media were supplemented with 10% fetal bovine serum and 100 IU/ml penicillin. Cells were seeded in 6-well plates at a density of 250,000 cells per well in complete medium, and 24 hr later, a stock solution of 8-MOP was added to the culture medium to render its final concentration 2.5 μM. The mixture was incubated at 37°C in dark for 30 min, and subsequently irradiated with UVA light at a dose of 2 J/cm^2, which was measured by a Mannix UV-340 light meter (Mannix Instrument Inc., New York, NY). The cells were then cultured at 37°C in complete medium for different time intervals to allow for lesion repair. Cells were then harvested and washed with PBS. Trypan blue exclusion assay showed that cell viability was greater than 90% at the end of the entire experiment. It is worth noting that 8-MOP could be rapidly absorbed after oral administration or penetrates into the epidermis and dermis following topical (cream or bath) application. The peak concentrations of 8-MOP in patient plasma and dermis are in the range of 45–970 ng/mL,[29–31] and the UVA dose employed for PUVA treatment is typically within the range of 1–10 J/cm^2.[32, 33] Thus, the concentration of 8-MOP (2.5 μM, or 540 ng/mL) and the dose of UVA irradiation (2 J/cm^2) used in this study were pharmacologically relevant.

DNA Extraction and Enzymatic Digestion

Genomic DNA was isolated from the resulting cell lysate using a high-salt method[34] and desalted by ethanol precipitation. The isolated DNA (10 μg in 100 μL ddH_2O) was subsequently mixed with 0.5 pmol of authentic D_3-8-MOP-ICL-carrying duplex ODN and 0.2 pmol of D_3-8-MOP-MA-containing ODN. To the mixture were added nuclease P1 (0.5 unit) and a 5-μL solution containing 300 mM sodium acetate (pH 5.6) and 10 mM zinc acetate. Nuclease P1 has combined endo- and exonuclease activities that can hydrolyze nucleic acid to 5′-mononucleotides. To prevent the potential loss of 5′ phosphate in the resulting nucleotides, a 5-μL phosphate buffer (10 mM, pH 5.7) was also added to the sample prior to the digestion. The digestion mixture was incubated at 37°C for 1 hr and extracted twice with chloroform to remove the enzyme. The aqueous layer was dried in a Speed-Vac concentrator, reconstituted in 20 μL H_2O, and a 5–15 μL aliquot was injected for LC-MS/MS analysis.

LC-MS/MS Analysis

The LC-MS/MS experiments were conducted on an LTQ linear ion-trap mass spectrometer (Thermo, San Jose, CA), and a 0.5×250 mm Zorbax SB-C18 column (5 μm in particle size, Agilent Technologies, Santa Clara, CA) was employed, as described previously [24, 25]. The flow rate was 8.0 $\mu L \cdot min^{-1}$, and a solution of 400 mM 1,1,1,3,3,3-hexafluoro-2-propanol (HFIP, pH was adjusted to 7.0 by addition of triethylamine, solution A) and methanol (solution B) were used as mobile phases for the separation of nucleotide mixtures arising from nuclease P1 digestion. A gradient of 5 min at 0% B, 5 min of 0–20% B, and 40 min of 20–50% B was employed for the separation. The mass spectrometer was set up to acquire the tandem mass spectra (MS/MS) for the fragmentation of the $[M-2H]^{2-}$ ions of tetranucleotides harboring ICL induced by 8-MOP or D_3-8-MOP and the $[M-H]^-$ ions of dinucleotides containing MAs formed from 8-MOP or D_3-8-MOP.

Calibration curves for the quantification of 8-MOP-ICL and 8-MOP-MAs were constructed by LC-MS/MS analysis of the nuclease P1 digestion products of standard ODN mixtures, which contained known amounts of the unlabeled 8-MOP-ICL- and -MA1-housing 12mer ODNs, together with 0.5 pmol D_3-8-MOP-ICL-bearing 12mer duplex ODN and 0.2 pmol 8-MOP-MA1-bearing single-stranded ODN. The LC-MS/MS experiments were conducted under identical conditions as described above for the nuclease P1-produced nucleotide mixture of cellular DNA.

Results and Discussion

Preparation of Standard ICL- and MA-containing ODNs

To examine the repair of 8-MOP-induced lesions in cells by LC-MS/MS, we first prepared ODNs bearing an ICL or MA induced by 8-MOP or D_3-8-MOP (Scheme 1A), the latter of which was synthesized previously [24]. After UVA exposure and photoreversal, we isolated the ICL-carrying duplex ODN and MA-bearing single-stranded ODNs from the mixture by HPLC. The 32.9-min fraction shown in Figure S1 was identified as 8-MOP-ICL in d(CGCGCTAGCGCG), and the fractions eluting at 27.5, 29.1, and 29.7 min were found to be the ODN carrying isomeric 8-MOP-MAs. The identities of the ICL- and MA-containing ODNs were further confirmed via mass spectrometric characterization after nuclease P1 digestion, and the amounts of the ODNs were quantified by UV absorption measurements at 260 nm.

Unlike a previously described method where mitomycin C crosslink-containing dinucleoside was employed as standard,[27] we chose to use stable isotope-labeled, lesion-carrying ODNs as standards because the standard ODNs are digested together with DNA isolated from 8-MOP-treated cells. Therefore, the assay allows for more accurate quantification of 8-MOP-ICL and -MAs in cellular DNA by accounting for potential incomplete release of ICL and MAs from DNA during the enzymatic digestion and potential loss of target analytes during other stages of sample preparation process.

Identification and Quantification of DNA ICL and MAs Induced by 8-MOP/UVA in Mammalian Cells

Previous studies revealed that ICL and MAs induced by different psoralen derivatives prevent the nuclease P1-mediated hydrolysis of the phosphodiester linkage between the crosslinked dT and its neighboring 3′ dA.[24, 35] Thus, nuclease P1 digestion facilitates the release of 8-MOP-induced ICL and MA from DNA as lesion-bearing tetranucleotide and dinucleotide, respectively (Scheme 1B). Indeed, negative-ion ESI-MS of the nuclease P1 digestion products of 8-MOP- and D_3-8-MOP-ICL-containing ODNs showed the ions of *m/z* 742 and 743.5, corresponding to the $[M-2H]^{2-}$ ions of 8-MOP- and D_3-8-MOP-ICL-

bearing tetranucleotide. Likewise, the MS of digestion mixtures of ODNs carrying both 8-MOP- and D_3-8-MOP-MA revealed the *m/z* 850 and 853 ions for the $[M-H]^-$ ions of 8-MOP- and D_3-8-MOP-MA-containing dinucleotide (data not shown).

By employing MS/MS, along with the use of authentic ODNs carrying the D_3-8-MOP lesions, we demonstrated that 8-MOP-induced ICL and MAs are readily detectable in human skin fibroblasts and CHO cells treated with 8-MOP and UVA light (representative LC-MS/MS results are shown in Figures 1 and 2, and the assignments for major fragment ions are depicted in Scheme 1C). Our LC-MS/MS method also allowed for the accurate quantification of 8-MOP-induced ICL and MAs in mammalian cells. In this respect, three peaks at 25.4, 28.2 and 30.5 min were observed in the SIC for the *m/z* 850 → 519 transition (Figure 2A), and according to their elution orders, these three MAs were designated as 8-MOP-MA1, -MA2 and -MA3, respectively. We assumed that the dinucleotides carrying the three isomeric MAs share the same ionization efficiency. This should be a reasonable assumption in the viewpoint that the deprotonated ions were monitored and the three MAs are structural isomers. Thus, we constructed only one calibration curve by analyzing the nuclease P1 digestion products of ODN mixtures containing D_3-8-MOP MA1 and its unlabeled counterpart at different molar ratios, and used this curve to quantify all three 8-MOP MAs formed in cells (Figure S2).

The limits of quantitation (LOQ) and limits of detection (LOD), defined as the amounts of analytes giving rise to signal-to-noise ratios of 10 and 3, were 33.3 fmol and 10.9 fmol for 8-MOP-ICL and 8-MOP-MA, respectively, and 10 fmol and 3.3 fmol for the ICL and MA, respectively. Although immunoassays can offer a sensitivity of detecting 17 fmol MAs in cells treated with 8-MOP,[36] the LC-MS/MS method that we developed here can facilitate the simultaneous quantification of 8-MOP ICL and MAs with the use of a relatively small amount (5 μg) of DNA. This level of sensitivity renders the method useful for assessing the repair of DNA adducts in mammalian cells.

Role of NER in the Cellular Repair of 8-MOP Photolesions

After demonstrating that ICL and MAs could be readily detected in HF and CHO cells after exposure to 8-MOP and UVA light, we next assessed their repair in these two types of cells. For these experiments, we employed a drug treatment and UVA irradiation condition that minimally perturbs the physiology and DNA repair capacity of the host cells. In particular, instead of dispersing the cells in PBS in previous experiments,[24, 25] we seeded the cells in the culture media during drug uptake and UVA light exposure. Additionally, the cells were not placed on ice during UVA exposure. With the use of these conditions, we found more than 90% viability of the cells at the end of the experimental period.

These experimental conditions, together with the use of LC-MS/MS, also allowed for examining the repair of 8-MOP-ICL and -MAs in mammalian cells. Our quantification results showed that, at 8 hr after photo-irradiation, the levels of 8-MOP-ICL in repair-proficient HF (GM00637) and CHO cells (CHO-AA8) decreased from 8.7 to 3.2 lesions and from 4.4 to 0 lesions per 10^6 nucleotides (Figure 3). However, cells deficient in XPA or ERCC1 failed to efficiently remove ICLs at 24 hr after 8-MOP had been photo-activated in these cells. For instance, ICL was detected at the level of 3.2 per 10^6 nucleotides in repair-competent GM00637 cells at 24 hr after 8-MOP/UVA treatment, while almost twice of that (5.7 ICLs per 10^6 nucleotides) was observed in XPA-deficient GM04429 cells (Figure 3A). The level of 8-MOP-ICL in ERCC1-deficient CHO cells also exhibited no significant change at 24 hr after irradiation, where the lesion remains at the level of 7.4 ICLs per 10^6 nucleotides (CHO-7–27, Figure 3B). These results also suggest that the dose of 8-MOP (2.5 μM) and UVA exposure (2.0 J/cm^2) did not compromise the repair capacity of the HF and CHO cells.

In the repair-proficient GM00637 cells, the level of 8-MOP-MA3 substantially declined from 47.7 to 12.3 adducts per 10^6 nucleotides at 24 hr after UVA exposure, which was accompanied with slight decreases of 8-MOP-MA1 and -MA2 (by 26% and 29%, respectively, Figure 4A, 4B, and 4C). On the other hand, repair-proficient CHO-AA8 cells exhibited a more efficient removal of the 8-MOP-MA lesions. The levels of all three MAs in AA8 cells decreased dramatically with time, with MA1 being hardly detectable in cells at 24 hr after UVA irradiation (CHO-AA8, Figure 4). In contrast, the XPA-deficient GM04429 cells and ERCC1-deficient CHO-7–27 cells displayed no apparent repair of any of the three MAs (Figure 4). These results demonstrated that the sensitivity, accuracy, and precision of the LC-MS/MS coupled with stable isotope dilution method facilitated the assessment of the repair of 8-MOP-induced ICL and MAs in mammalian cells. Although others and we previously employed LC-MS/MS for detecting DNA ICLs in cells or tissues [24–27], to our knowledge, this is one of the first few reports about the application of LC-MS/MS for examining the repair of any DNA ICLs.[27]

The ERCC1-XPF complex is a structure-specific endonuclease that functions in NER by cleaving damaged strand at the 5′ side to the lesion.[37] Previous studies showed that, unlike yeast where loss of any of the several NER proteins confers sensitivity to crosslinking agents, only elimination of ERCC1 or XPF leads to exquisite sensitivity of mammalian cells toward these agents.[38, 39] In comparison, the increase in sensitivity to crosslinking agents was observed to be more modest with mutations in XPA, another NER protein involved in damage recognition.[40] However, even if XPA is not required for the repair of an ICL substrate *in vitro*,[41] failure to complete the repair step by XPA renders the ICLs persistent in cells and is at least cytostatic.[40] Additionally, Niedernhofer et al.[42] found that XPA-mutant primary HFs are more sensitive than normal controls to mitomycin C, a potent DNA crosslinker. In support of these previous notions, our results provided direct evidence to demonstrate that XPA and ERCC1 are both required for the efficient repair of 8-MOP-ICL in mammalian cells, as reflected by the elevated accumulation of 8-MOP-ICL in mammalian cells deficient in one of these two genes. A similar finding was made for 8-MOP-MAs, underscoring the involvement of NER pathway in the repair of these psoralen-induced MAs.

It is of note that there is substantial functional overlap among the proteins in the various pathways for complete processing of bulky DNA damage. For example, recent studies suggested that NEIL1-mediated base excision repair (BER) may also be involved in the repair of ICLs induced by 8-MOP/UVA.[43, 44] Therefore, it is important to assess, in the future, the roles of other DNA repair pathways in the removal of psoralen ICLs in mammalian cells. It can be envisaged that the analytical method developed here can be readily employed for such studies.

Removal efficiency of 8-MOP-Induced DNA Lesions in Different Cell Types

The LC-MS/MS results also allowed us to compare the relative repair efficiencies of 8-MOP photoproducts in different cell types. The overall level of 8-MOP-ICL was found to be approximately 1.6-fold higher in HFs than in CHO cells obtained after UVA photoactivation. In addition, we observed that, at 8 hr post irradiation, 19% and 40% of the 8-MOP-ICL were removed in repair-proficient HF (GM00637) and CHO (CHO-AA8) cells, respectively (Figure 3). We also examined, by using the same method, the repair of 8-MOP photoadducts in 293T human embryonic kidney epithelial (HEK293T) cells. Interestingly, the yield of 8-MOP-ICL in HEK293T cells was below the detection limit, indicating that the lesion is much more rapidly repaired in this type of cells than in HFs and CHO cells (Figure S3). Similarly, the rates of removal of 8-MOP-introduced MAs in three types of cells followed the same trend as that of the ICL, where the MA processing rate in repair-competent CHO cells was 1.5–2.0-fold higher than that in HFs, but markedly lower than that in HEK293T cells. This result shows that the removal of psoralen photoadducts of DNA in

mammalian cells is cell type-specific. Similar observation was made for other types of DNA lesions. For instance, D'Errico et al. [45] showed that lower levels of UV photoproducts are induced in keratinocytes relative to fibroblasts under the same UV dose regimen.

Conclusions

The goal of the present work was to develop an LC-MS/MS method for assessing the repair of DNA damage induced by psoralen and UVA light in mammalian cells. Our results demonstrated that the unequivocal chemical specificity, accuracy, sensitivity, and reproducibility of the LC-MS/MS coupled with isotope dilution technique allowed for monitoring the repair of 8-MOP-induced ICL and MAs in mammalian cells. With the use of this method, we investigated the impact of defective NER pathway on the cellular removal of 8-MOP/UVA-induced DNA damage by comparing HFs derived from normal and XPA individuals, and CHO cells that are repair-competent or deficient in ERCC1. The results revealed a much lower removal rate of ICL and MAs in repair-deficient mammalian cells relative to their repair-competent counterparts, thereby providing direct evidence to unambiguously support the role of NER in repairing these DNA lesions. It can be envisaged that the method can be generally applicable for examining the roles of other DNA repair enzymes and pathways in removing these lesions in mammalian cells.

The nuclease P1 digestion combined with LC-MS/MS method should be generally useful for monitoring the repair of other ICLs in mammalian cells. Along this line, a previous X-ray crystal structure study of nuclease P1-DNA complex unveiled that the nucleobase on the 5′ side of the phosphodiester bond to be cleaved has to fit into the binding pocket close to the active site of the enzyme and forms π stacking interaction with the phenylalanine residue in the binding pocket.[46] Thus, any ICLs in which the crosslinked nucleobase loses its aromaticity or becomes bulky will not be able to fit into the active site of the enzyme, thereby preventing the 3′ phosphodiester bond from nuclease P1 cleavage. Indeed we observed that the crosslink-bearing tetranucleotide could also arise from cleavage of duplex DNA harboring a mitomycin C-induced ICL formed between two guanine residues at CpG site or an ICL formed between an abasic site and guanine.[35, 47]

Our LC-MS/MS method also unveiled variations in repair efficiencies among the three types of mammalian cells (i.e., HFs, CHO cells and human embryonic kidney epithelial cells), suggesting that the method may also be useful for examining the repair capacities of different individuals toward these DNA lesions. Such a possibility is also manifested by the fact that pharmacologically relevant doses of 8-MOP and UVA light were used in the present study. Thus, our LC-MS/MS-based approach may facilitate the future use of ICL and MAs as biomarkers for defining the optimal dose of PUVA treatment in individual patients.

In summary, we reported, for the first time, a mass spectrometry-based approach for monitoring simultaneously the repair of psoralen-induced ICL and MAs in mammalian cells. This also constitutes one of the first few applications of LC-MS/MS for examining the repair of any DNA ICLs in general.

Supplementary Material

Refer to Web version on PubMed Central for supplementary material.

Acknowledgments

The authors would like to thank Dr. Huachuan Cao for synthesizing D_3-8-MOP, and Profs. Gerd P. Pfeifer and Michael M. Seidman for providing cell lines. This work was supported by the National Institutes of Health (R01 ES019873 and R01 ES021007).

Abbreviations

8-MOP	8-methoxypsoralen
ICL	interstrand crosslink
MA	monoadduct
ODN	oligodeoxyribonucleotide
HF	human fibroblast
CHO	Chinese hamster ovary
XPA	xeroderma pigmentosum, complementation group A
ERCC1	excision repair cross-complementing rodent repair deficiency, complementation group 1
ESI-MS	electrospray ionization-mass spectrometry
MS/MS	tandem MS

References

1. Lindahl T. Nature. 1993; 362:709–715. [PubMed: 8469282]
2. Friedberg, EC.; Walker, GC.; Siede, W.; Wood, RD.; Schultz, RA.; Ellenberger, T. DNA Repair and Mutagenesis. 2. American Society for Microbiology Press; Washington D.C: 2006.
3. Lindahl T, Barnes DE. Cold Spring Harb Symp Quant Biol. 2000; 65:127–133. [PubMed: 12760027]
4. Dronkert ML, Kanaar R. Mutat Res. 2001; 486:217–247. [PubMed: 11516927]
5. Muniandy PA, Liu J, Majumdar A, Liu ST, Seidman MM. Crit Rev Biochem Mol Biol. 2010; 45:23–49. [PubMed: 20039786]
6. Deans AJ, West SC. Nat Rev Cancer. 2011; 11:467–480. [PubMed: 21701511]
7. McCabe KM, Olson SB, Moses RE. J Cell Physiol. 2009; 220:569–573. [PubMed: 19452447]
8. Wood RD. Environ Mol Mutagen. 2010; 51:520–526. [PubMed: 20658645]
9. Noll DM, Mason TM, Miller PS. Chem Rev. 2006; 106:277–301. [PubMed: 16464006]
10. Hearst JE. Chem Res Toxicol. 1989; 2:69–75. [PubMed: 2519712]
11. Stern RS. N Engl J Med. 2007; 357:682–690. [PubMed: 17699818]
12. Dalla Via L, Marciani Magno S. Curr Med Chem. 2001; 8:1405–1418. [PubMed: 11562274]
13. Nijsten TE, Stern RS. J Invest Dermatol. 2003; 121:252–258. [PubMed: 12880415]
14. Hlavin EM, Smeaton MB, Miller PS. Environ Mol Mutagen. 2010; 51:604–624. [PubMed: 20658650]
15. Zheng H, Wang X, Legerski RJ, Glazer PM, Li L. DNA Repair. 2006; 5:566–574. [PubMed: 16569514]
16. Pospisilova S, Kypr J. Photochem Photobiol. 1997; 65:945–948. [PubMed: 9188274]
17. Lee CS, Gibson NW. Cancer Res. 1991; 51:6586–6591. [PubMed: 1742731]
18. Hartley JM, Spanswick VJ, Gander M, Giacomini G, Whelan J, Souhami RL, Hartley JA. Clin Cancer Res. 1999; 5:507–512. [PubMed: 10100700]
19. Hartley JA, Souhami RL, Berardini MD. J Chromatogr. 1993; 618:277–288. [PubMed: 8227260]

20. Courdavault S, Baudouin C, Charveron M, Canguilhem B, Favier A, Cadet J, Douki T. DNA Repair. 2005; 4:836–844. [PubMed: 15950551]
21. Harrington CF, Le Pla RC, Jones GDD, Thomas AL, Farmer PB. Chem Res Toxicol. 2010; 23:1313–1321. [PubMed: 20666396]
22. Wang J, Cao H, You C, Yuan B, Bahde R, Gupta S, Nishigori C, Niedernhofer LJ, Brooks PJ, Wang Y. Nucleic Acids Res. 2012; 40:7368–7374. [PubMed: 22581771]
23. Wang J, Clauson CL, Robbins PD, Niedernhofer LJ, Wang Y. Aging Cell. 2012; 11:714–716. [PubMed: 22530741]
24. Cao H, Hearst JE, Corash L, Wang Y. Anal Chem. 2008; 80:2932–2938. [PubMed: 18324836]
25. Lai C, Cao H, Hearst JE, Corash L, Luo H, Wang Y. Anal Chem. 2008; 80:8790–8798. [PubMed: 18947205]
26. Malayappan B, Johnson L, Nie B, Panchal D, Matter B, Jacobson P, Tretyakova N. Anal Chem. 2010; 82:3650–3658. [PubMed: 20361772]
27. Paz MM, Ladwa S, Champeil E, Liu Y, Rockwell S, Boamah EK, Bargonetti J, Callahan J, Roach J, Tomasz M. Chem Res Toxicol. 2008; 21:2370–2378. [PubMed: 19053323]
28. Rolig RL, Layher SK, Santi B, Adair GM, Gu F, Rainbow AJ, Nairn RS. Mutagenesis. 1997; 12:277–283. [PubMed: 9237774]
29. von Kobyletzki G, Hoffmann K, Kerscher M, Altmeyer P. Photodermatol Photoimmunol Photomed. 1998; 14:136–138. [PubMed: 9779504]
30. Thomas SE, O'Sullivan J, Balac N. Br J Dermatol. 1991; 125:56–58. [PubMed: 1873204]
31. Tegeder I, Brautigam L, Podda M, Meier S, Kaufmann R, Geisslinger G, Grundmann-Kollmann M. Clin Pharmacol Ther. 2002; 71:153–161. [PubMed: 11907489]
32. Tanew A, Kipfelsperger T, Seeber A, Radakovic-Fijan S, Honigsmann H. J Am Acad Dermatol. 2001; 44:638–642. [PubMed: 11260539]
33. Yeo UC, Shin JH, Yang JM, Park KB, Kim MM, Bok HS, Lee ES. Br J Dermatol. 2000; 142:733–739. [PubMed: 10792224]
34. Miller SA, Dykes DD, Polesky HF. Nucleic Acids Res. 1988; 16:1215. [PubMed: 3344216]
35. Wang Y, Wang Y. Anal Chem. 2003; 75:6306–6313. [PubMed: 14616015]
36. Gasparro FP. J Photochem Photobiol B. 1988; 2:286–288. [PubMed: 3149996]
37. Evans E, Moggs JG, Hwang JR, Egly JM, Wood RD. EMBO J. 1997; 16:6559–6573. [PubMed: 9351836]
38. De Silva IU, McHugh PJ, Clingen PH, Hartley JA. Mol Cell Biol. 2000; 20:7980–7990. [PubMed: 11027268]
39. Usanova S, Piee-Staffa A, Sied U, Thomale J, Schneider A, Kaina B, Koberle B. Mol Cancer. 2010; 9:248. [PubMed: 20846399]
40. Bergstralh DT, Sekelsky J. Trends Genet. 2008; 24:70–76. [PubMed: 18192062]
41. Cipak L, Watanabe N, Bessho T. Nat Struct Mol Biol. 2006; 13:729–733. [PubMed: 16845393]
42. Niedernhofer LJ, Garinis GA, Raams A, Lalai AS, Robinson AR, Appeldoorn E, Odijk H, Oostendorp R, Ahmad A, van Leeuwen W, Theil AF, Vermeulen W, van der Horst GT, Meinecke P, Kleijer WJ, Vijg J, Jaspers NG, Hoeijmakers JH. Nature. 2006; 444:1038–1043. [PubMed: 17183314]
43. Couve S, Mace-Aime G, Rosselli F, Saparbaev MK. J Biol Chem. 2009; 284:11963–11970. [PubMed: 19258314]
44. Couve-Privat S, Mace G, Rosselli F, Saparbaev MK. Nucleic Acids Res. 2007; 35:5672–5682. [PubMed: 17715144]
45. D'Errico M, Teson M, Calcagnile A, Nardo T, De Luca N, Lazzari C, Soddu S, Zambruno G, Stefanini M, Dogliotti E. Cancer Res. 2005; 65:432–438. [PubMed: 15695384]
46. Romier C, Dominguez R, Lahm A, Dahl O, Suck D. Proteins. 1998; 32:414–424. [PubMed: 9726413]
47. Johnson KM, Price NE, Wang J, Fekry MI, Dutta S, Seiner DR, Wang Y, Gates KS. J Am Chem Soc. 2013; 135:1015–1025. [PubMed: 23215239]

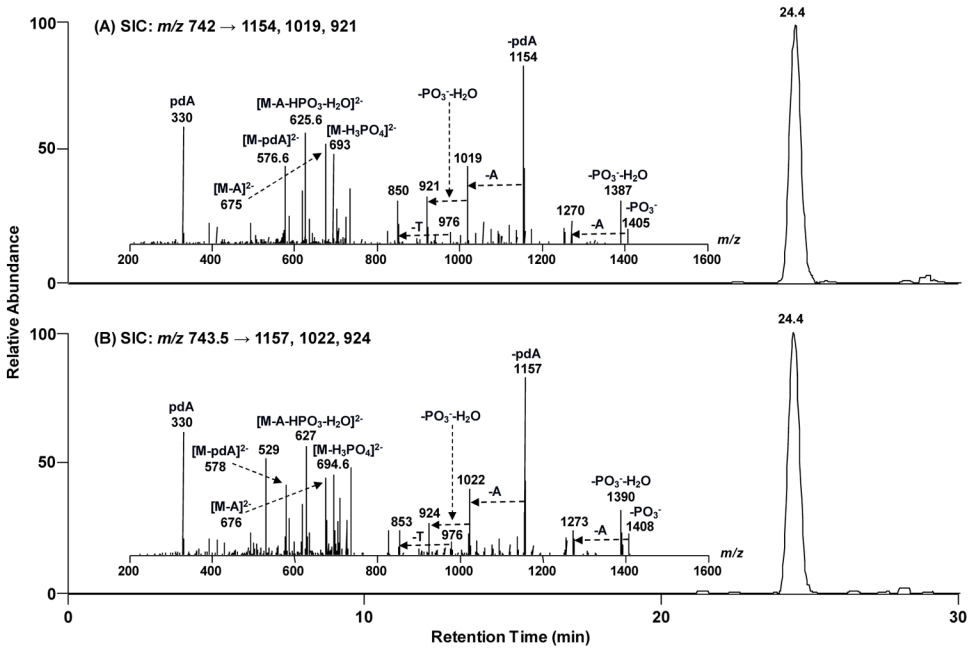

Figure 1.

Selected-ion chromatograms (SICs) for monitoring the *m/z* 742.0→1154, 1019, 921 transitions for 8-MOP-ICL-containing tetranucleotide (A) and the *m/z* 743.5→1157, 1022, 924 transitions for D_3-8-MOP-ICL-containing tetranucleotide (B) resulting from nuclease P1 digestion of DNA extracted from wild-type CHO cells immediately after photoirradiation (i.e., at 0 hr). Shown in the insets are the product-ion spectra of the ESI-produced $[M-2H]^{2-}$ ions of the tetranucleotide housing unlabeled and labeled 8-MOP-ICL.

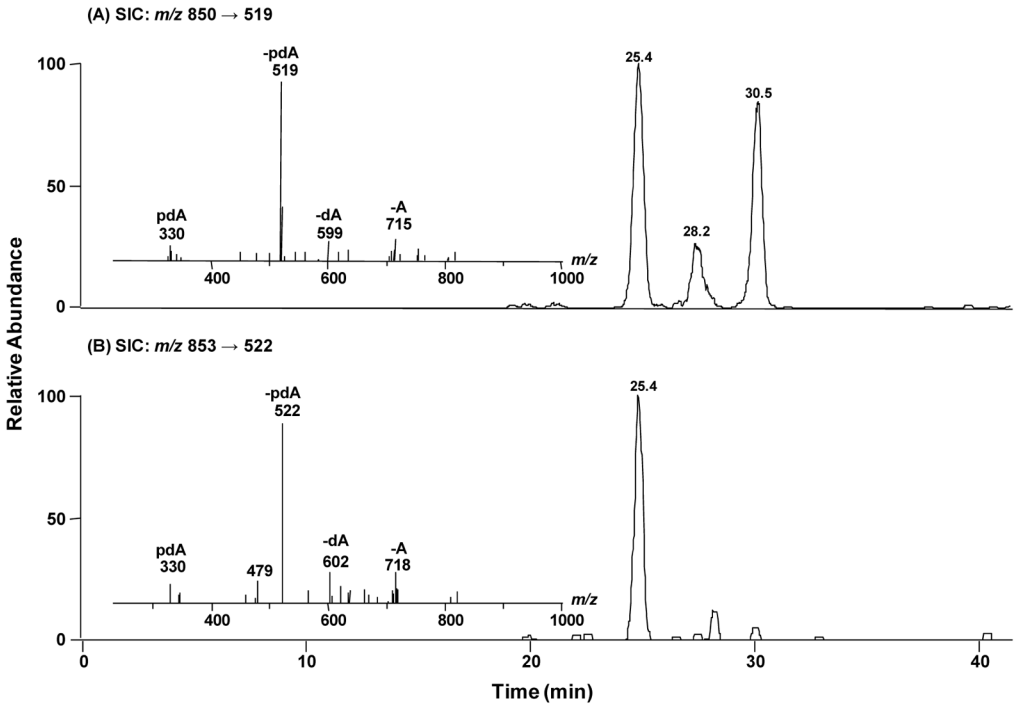

Figure 2.

Selected-ion chromatograms (SICs) for monitoring the *m/z* 850→519 transition for 8-MOP-MA-containing dinucleotides (A) and the *m/z* 853→522 transition for D_3-8-MOP-MA-containing dinucleotide (B) resulting from nuclease P1 digestion of DNA extracted from wild-type CHO cells immediately after photoirradiation (i.e., at 0 hr). Shown in the insets are the product-ion spectra of the ESI-produced $[M-H]^-$ ions of the dinucleotide containing unlabeled and labeled 8-MOP-MA.

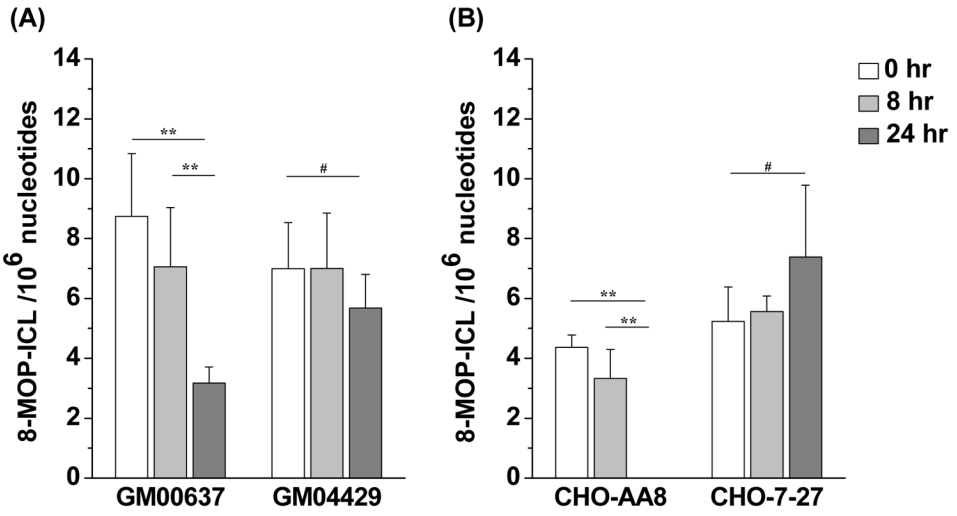

Figure 3.

LC-MS/MS quantification results for 8-MOP-ICLs in DNA samples from human skin fibroblast (A) and Chinese hamster ovary cells (B). Data represent the means and standard deviations of results obtained from three independent experiments. *, $p < 0.05$; **, $p < 0.01$; #, $p > 0.05$. The p-values were calculated by using unpaired two-tailed t-test.

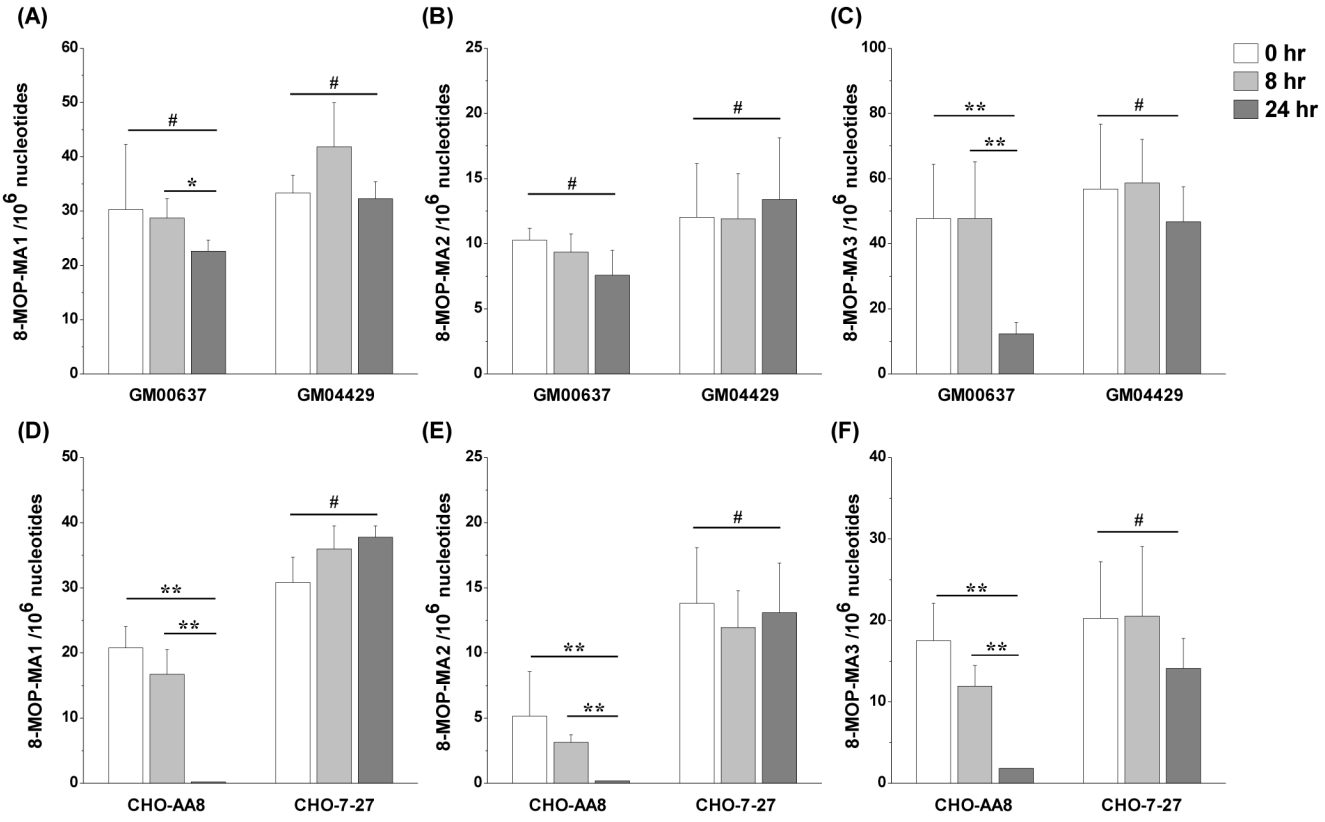

Figure 4.

LC-MS/MS quantification results for 8-MOP-MAs in DNA samples. The results for MA1, MA2, and MA3 in human skin fibroblast cells are shown in (A), (B), and (C), respectively. The corresponding data for Chinese hamster ovary cells are displayed in (D), (E), and (F), respectively. The data represent the means and standard deviations of results obtained from three independent experiments. *, $p < 0.05$; **, $p < 0.01$; #, $p > 0.05$. The *p*-values were calculated by using unpaired two-tailed *t*-test.

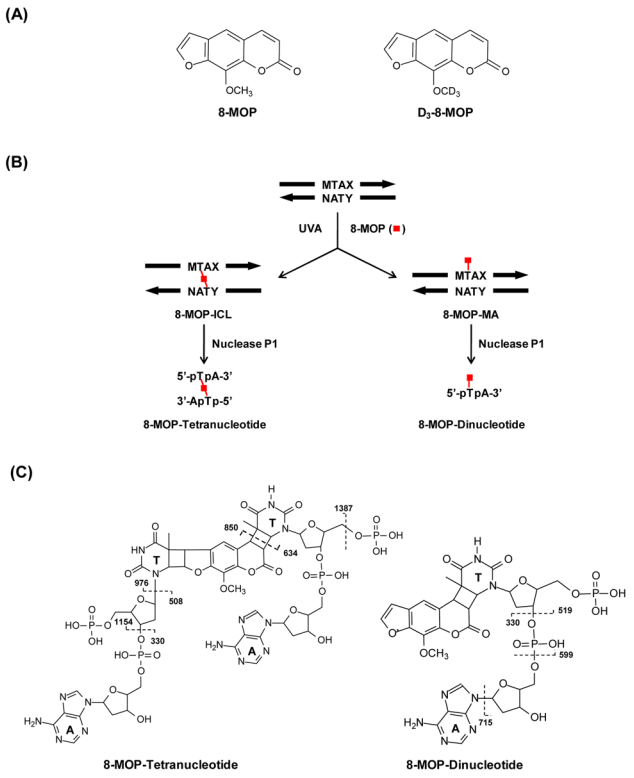

Scheme 1.

(A) The chemical structures of 8-MOP and D_3-8-MOP; (B) Experimental outline of the enzymatic digestion of 8-MOP-ICL and 8-MOP-MAs in ODNs or cellular DNA; (C) The chemical structures of the tetranucleotide and dinucleotide generated from nuclease P1 digestion and the cleavages for the formation of major fragment ions observed in MS/MS.